

RESIDUAL SOILS

1. INTRODUCTION

Because residual soils weather from parent bedrock, the soil profile represents a history of the weathering process. Profile classification systems distinguish states of weathering and separate the profile vertically into different zones. The permeability and shear strength gradually change with depth, which controls both the local seepage response to rainfall infiltration and the location of the shear surface. Soil profile thickness and properties depend upon parent bedrock, discontinuities, topography, and climate. Because these factors vary horizontally, the profile can vary significantly over relatively short horizontal distances. In addition, deep profiles form in tropical regions where weathering agents are especially strong and the advanced stages of chemical weathering form cemented soils called laterites. Technical papers often refer to both tropical soils and residual soils. In this chapter general characteristics of residual soils are considered and illustrated with examples drawn from Brazil, Hong Kong, and North Carolina.

Figure 19-1 shows the typical weathering profiles that develop over igneous and metamorphic rocks labeled according to Deere and Patton's (1971) profile classification system, which divides the profile into three zones: *residual soil*, *weathered rock*, and *unweathered rock*. In addition, Deere and Patton present 12 other weathering-profile classification systems proposed by workers from other regions. For example, Brand (1985) divided Hong

Kong soils into six material grades and four profile zones.

In 1990 a working party of the Engineering Group of the Geological Society of London issued an extensive report entitled *Tropical Residual Soils* (Geological Society of London 1990), which proposed the classification of tropical residual soils presented in Figure 19-2. This classification contains a series of grades identified by roman numerals I through VI. Comparison of the Deere and Patton classification (Figure 19-1) with the Geological Society of London working party classification (Figure 19-2) reveals the potential for significant confusion. Both classifications use roman numerals to identify different portions of the weathering profile. However, Deere and Patton use roman numeral I to identify the most intensely weathered material at the top of the profile, whereas the working party uses roman numeral I to define fresh rock at the base of the profile. Obviously the "grades" of the working party and the "zones" of Deere and Patton attempt to define the same phenomena.

In this chapter Deere and Patton's system as defined in Figure 19-1 will be used exclusively, although it is recognized that other systems, such as the classification by the Geological Society of London working party defined in Figure 19-2, may work better in some regions. Papers describing landslides in residual soils often spend more time qualitatively describing the profile and the horizontal variability than in quantitatively reporting mea-

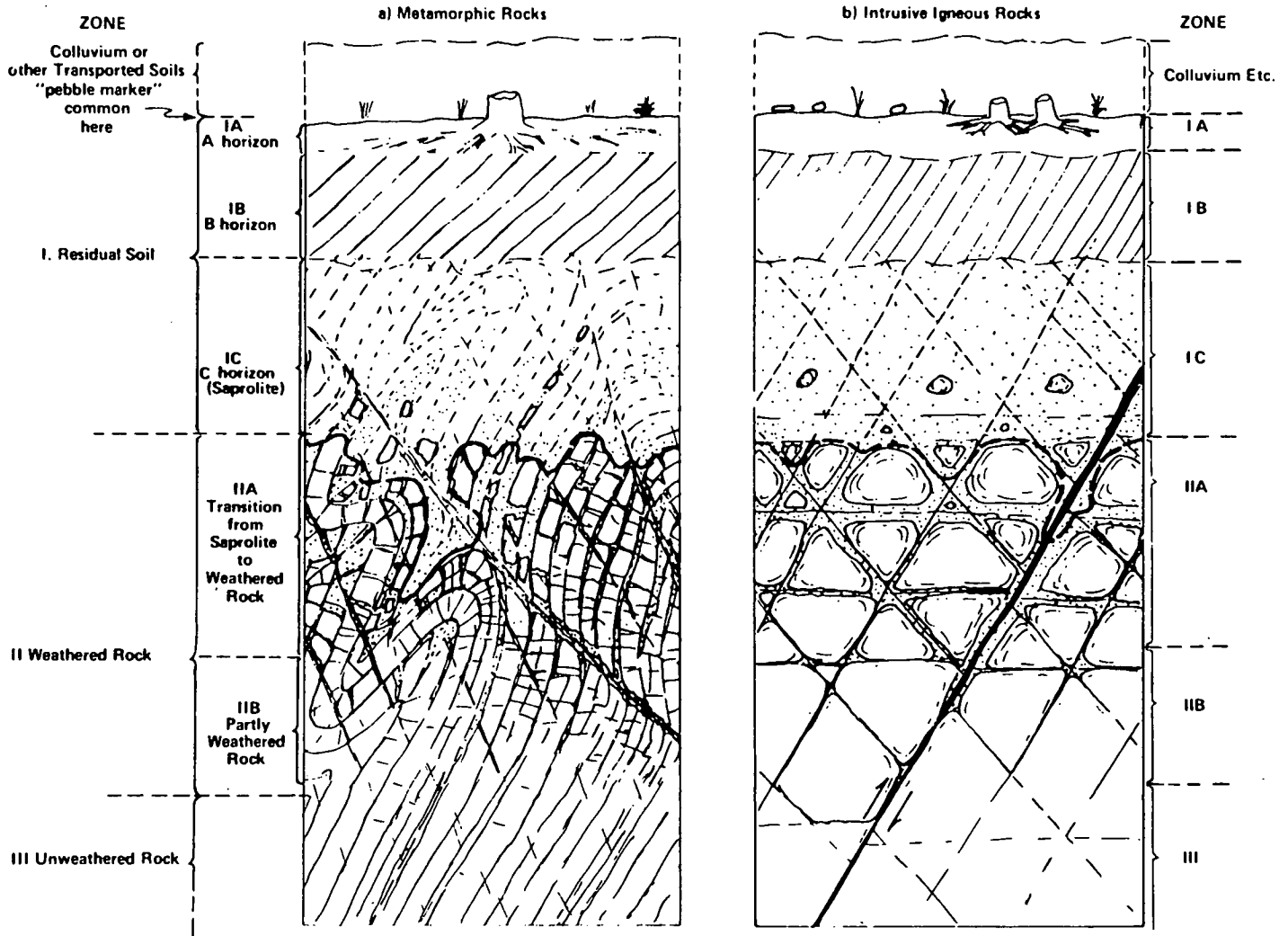


FIGURE 19-1
Typical weathering
profile for
metamorphic and
igneous rocks
(Deere and Patton
1971).

REPRINTED WITH
PERMISSION OF
AMERICAN SOCIETY OF
CIVIL ENGINEERS

sured pore pressures and shear-strength parameters. Brand (1985) concluded that the ability to predict the performance of slopes in residual soils is only poor to fair.

Table 19-1 shows the relative permeability and shear strength for materials within different weathering profile zones as defined by Deere and Patton (1971). The subdivision of Zone I, residual soil, into A, B, and C horizons follows the convention used by soil scientists who study weathering processes in the formation of soils. Soils in A and B horizons have experienced significant chemical weathering that results in a breakdown of rock into silt- and clay-sized particles. Rainfall infiltration leaches chemicals from the A horizon, which then accumulate in the B horizon. Because weathering has removed most traces of bedrock

structure, the soils in these horizons resemble the silty clays, sandy silts, and silty sands found in transported soils. Soils in horizon C, or saprolite, behave differently than transported soils do. Deere and Patton emphasized that the profile classification has to be added to more traditional soil classifications during exploration. Generally, unambiguous classification requires continuous sampling or inspection of open cuts in test pits or road cuts. Brand and Phillipson (1985) provided a good overview of practices used around the world to sample and test residual soils.

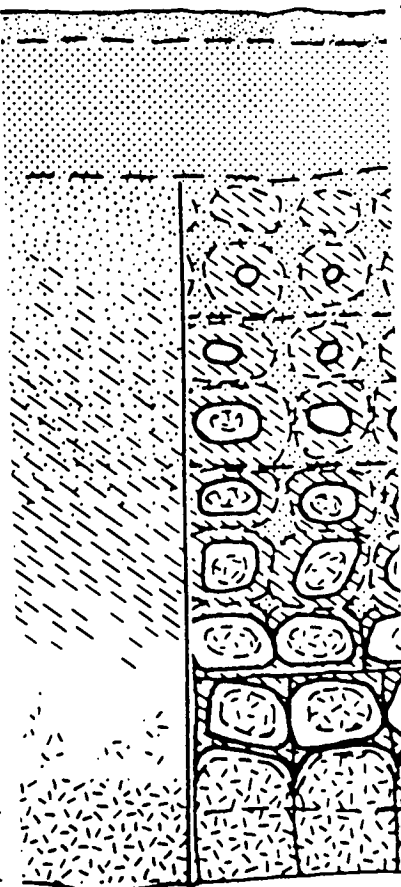
Saprolites retain the structure of parent bedrock, but with only a trace of the original bond strength. De Mello (1972) suggested that standard soil properties tests performed on thoroughly mixed specimens do not effectively represent

A. Defined idealized weathering profiles - without corestones (left) and with corestones (right).

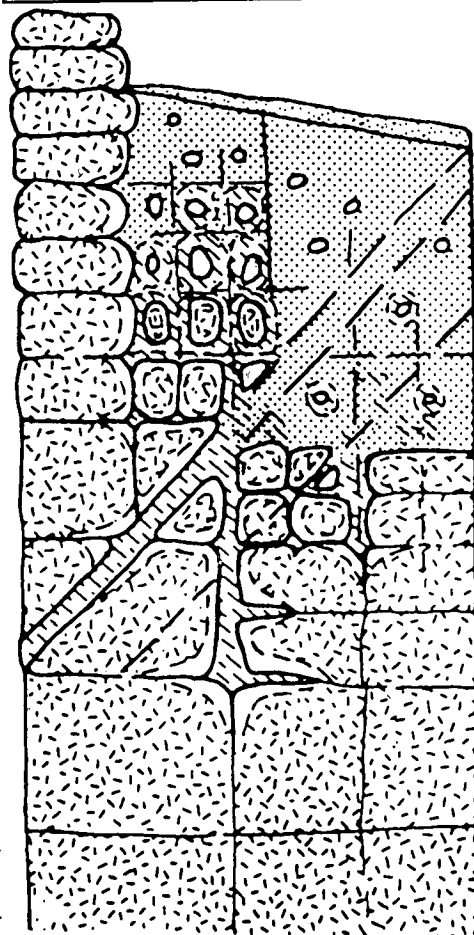
B. Descriptions of characteristics of the idealized profiles.

C. Example of a complex profile with corestones

Humus/topsoil
 VI
 Residual soil
 V
 Completely weathered
 IV
 Highly weathered
 III
 Moderately weathered
 II
 Slightly weathered
 IB Faintly weathered
 IA Fresh



Humus and topsoil
 All rock material converted to soil; mass structure and material fabric destroyed. Significant change in volume.
 All rock material decomposed and/or disintegrated to soil. Original mass structure still largely intact.
 More than 50% of rock material decomposed and/or disintegrated into soil. Fresh/discolored rock present as discontinuous framework or corestones.
 Less than 50% of rock material decomposed and/or disintegrated into soil. Fresh/discolored rock present as continuous framework or corestones.
 Discoloration indicates weathering of rock material and discontinuity surfaces. All rock material may be discolored by weathering and may be weaker than in its fresh condition.
 Discoloration on major discontinuity surfaces.
 No visible sign of rock material weathering.



LEGEND



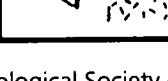
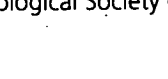
	Rock decomposed to soil
	Weathered/disintegrated rock
	Rock discolored by weathering
	Fresh rock

FIGURE 19-2 Tropical residual soil classification proposed by Geological Society of London working party (Geological Society of London 1990).

Table 19-1
Description of Weathering Profile for Igneous and Metamorphic Rocks (modified from Deere and Patton 1971)

ZONE	DESCRIPTION	ROCK QUALITY DESIGNATION ^a (NX CORE %)	PERCENT CORE RECOVERY ^b (NX CORE)	RELATIVE PERMEABILITY	RELATIVE STRENGTH
I, Residual soil					
IA, A Horizon	Topsoil, roots, organic material; zone of leaching and eluviation; may be porous	Not applicable	0	Medium to high	Low to medium
IB, B Horizon	Characteristically clay enriched; also accumulation of Fe, Al, and Si; hence may be cemented; no relict structures present	Not applicable	0	Low	Commonly low (high if cemented)
IC, C Horizon (saprolite)	Relict rock structures retained; silty grading to sandy material; less than 10% core stones: often micaceous	0 or not applicable	Generally 0-10	Medium	Low to medium (relict structures very significant)
II, Weathered rock					
IIA, Transition	Highly variable, soil-like to rocklike; fines commonly fine to coarse sand (gruss); 10 to 90% core stones; spheroidal weathering common	Variable, generally 0-50	Variable, generally 10-90	High	Medium to low where weak and relict structures present
IIB, Partly weathered rock (PWR)	Rocklike soft to hard rock; joints stained to altered; some alteration of feldspars and micas	Generally 50-75	Generally 90	Medium to high	Medium to high ^b
III, Unweathered rock	No iron stains to trace along joints; no weathering of feldspars or micas	Over 75 (generally 90)	Generally 100	Low to medium	Very high ^b

^a The descriptions provide the only reliable means of distinguishing the zones.

^b Only intact rock masses with no adversely oriented geologic structures.

saprolite soil properties. Both Sowers (1954, 1963) and Vaughan (1985a) have correlated properties to void ratio rather than to Atterberg limits because the void ratio represents the in situ state. Figure 19-1 shows that saprolites also retain relict discontinuities or joints present in parent bedrock. These discontinuities significantly influence the permeability and shear strength of the soil mass. In some cases laboratory-sized specimens provide misleading permeability coefficients and shear strengths. In addition, highly micaceous residual soils derived from gneisses expand elasti-

cally when unloaded during sampling. This expansion breaks weak bonds and decreases the soil's laboratory-measured shear strength and stiffness (Bressani and Vaughan 1989).

Zone IIA, or upper weathered-rock zone, provides a transition from saprolite to partly weathered rock (PWR). In Zone IIA the soil becomes progressively coarser with depth and has more core stones and clearer discontinuities. Although arbitrary boundaries separate different zones, the profile exhibits trends in changing properties. Zone IIA materials are described as soils, but it is

difficult to provide undisturbed samples of them for laboratory strength and permeability testing. Stability analyses of residual soil slopes fall in the continuum between soil mechanics and rock mechanics. Saprolites behave like soils but often slide along discontinuities. In contrast, Zone IIA transition materials exhibit both rocklike and soil-like properties. Since Zone IIA materials often have higher permeabilities than the overlying saprolites, they influence seepage in cut slopes.

Slopes composed of materials classified as Zone IIB (PWR) and Zone III (unweathered rock) are best treated as rock slopes. The depth of the boundary between Zones IIB and III significantly influences the cost of excavation in residual soil (White and Richardson 1987).

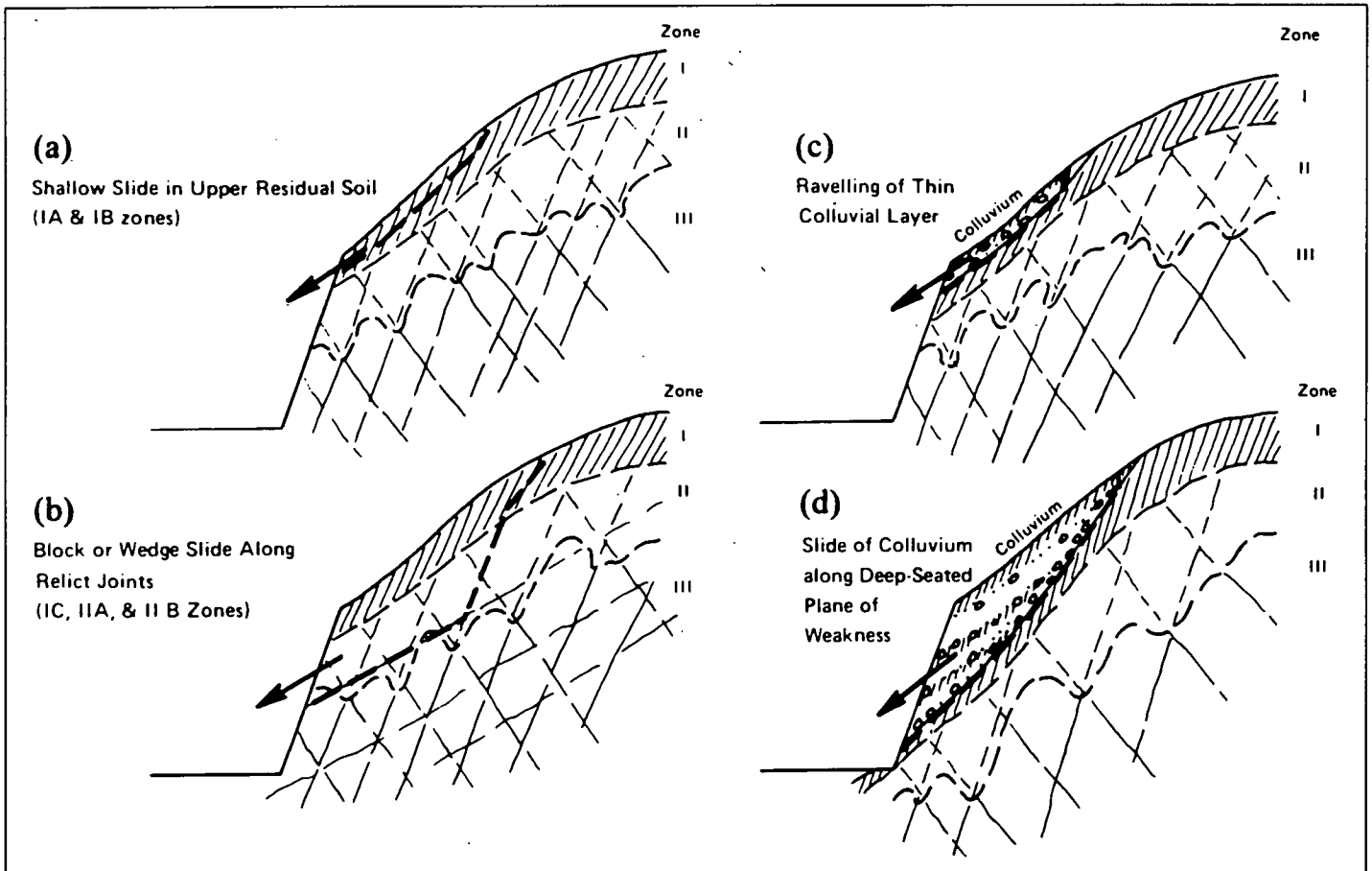
Figure 19-3 shows four common landslide types found in residual soil slopes (Deere and Patton 1971). Generally, investigations in specific regions identify and classify the common landslide types; Deere and Patton's classification system provides a general framework. Type *a* landslides

occur primarily in shallow Zone IA and IB soils, where colluvium from previous landslides has not covered the profile. Landslides frequently occur during heavy rainfall, and the saturated soil often moves as debris flows or mud flows. Jones (1973) described how many Type *a* landslides killed more than 1,700 people during heavy rainfall in January 1967 in the Serra das Araras region of Brazil. Type *b* landslides fail along relict joints located in Zone IC (saprolite), Zone IIA (transition), or Zone IIB (PWR). The joint pattern controls the shape of the landsliding mass. Although rainfall significantly influences pore pressures, landsliding can occur well after heavy rains when two- or three-dimensional seepage causes slope failures. In contrast, vertical infiltration of rainfall is the most frequent cause of shallow Type *a* and *b* landslides.

Type *c* and *d* landslides resemble Type *a* and *b* landslides but occur in colluvium-covered weathered profiles. In these residual soil profiles, the overlying colluvium usually resembles the texture of the underlying residual materials but lacks the

FIGURE 19-3 Common types of landslides in weathered rock, residual soil, and colluvium (Deere and Patton 1971).

REPRINTED WITH PERMISSION OF AMERICAN SOCIETY OF CIVIL ENGINEERS



rocklike structure and relict joints. Previous landslide mixes the colluvium with cobbles and core stones, making sampling difficult. Type *c* landslides differ little from Type *a* landslides except that the material properties are harder to measure. For Type *d* landslides, the colluvial cover significantly influences seepage. At the Boone landslide in North Carolina, described in Section 4.3, the colluvium had a higher permeability than the underlying saprolite. In contrast, at the Balsam Gap landslide, also in North Carolina, the colluvium had a lower permeability and acted as a low-permeability cap. Mapping the colluvium thickness provides a useful description of the horizontal variability controlling both current seepage and historical slide activity. Brand (1985) found that engineers often classify colluvium as residual soil.

Deere and Patton's classification system considers only cut slopes in residual soil profiles. Frequently, highway construction requires fill slopes over residual soils. Lumb (1975) included fill slopes placed upon residual soil slopes as one common and particularly dangerous landslide type in Hong Kong. Generally, residual soils have much higher values for in-place mass permeabilities than the same materials have once they have been transported, mixed, and compacted. Therefore, compacted fills often act as low-permeability caps, disrupting the natural seepage pattern and increasing pore pressures. The resulting landslides resemble Deere and Patton's Type *d* landslides, but in these cases the fill acts as the overlying colluvium.

2. SAPROLITE PROPERTIES

The stability of A and B horizon soils in Zone I may be effectively assessed by traditional soil mechanics analysis methods. The stability of Zone IIB (PWR) and Zone III (unweathered rock) materials may be effectively assessed by rock mechanics analysis methods. However, saprolite and transition materials fall in the continuum between soil mechanics and rock mechanics. Core stones make sampling difficult, and laboratory-sized specimens sometimes provide poor estimates of mass strength and permeability. The soil behavior described in this section refers primarily to saprolites but also applies to the soil matrix in transition soils.

Saprolites are generally unsaturated, weakly bonded, and heterogeneous soils with relict joint systems. Mitchell and Sitar (1982) reviewed the

engineering properties of tropical soils, qualitatively defined six stages of weathering, and described the corresponding changes in mineralogy and soil properties. Vaughan et al. (1988) reported that bond strength and void ratio control behavior of residual soils and that geologic origins of these soils cause the following primary characteristics:

1. The bonding derived from soil evolution and found at equilibrium with the current in situ stress state influences the soil's strength and stiffness,
2. The stress history during soil formation has little effect on the soil's current properties,
3. Soils have widely varying mineralogy and grain strength, and
4. In situ soils have widely varying void ratios.

Vaughan et al. (1988) experimentally examined the behavior of weakly bonded soils by artificially manufacturing test soils from a quartz and kaolin sand mixed with kaolin slurry and then fired in a furnace.

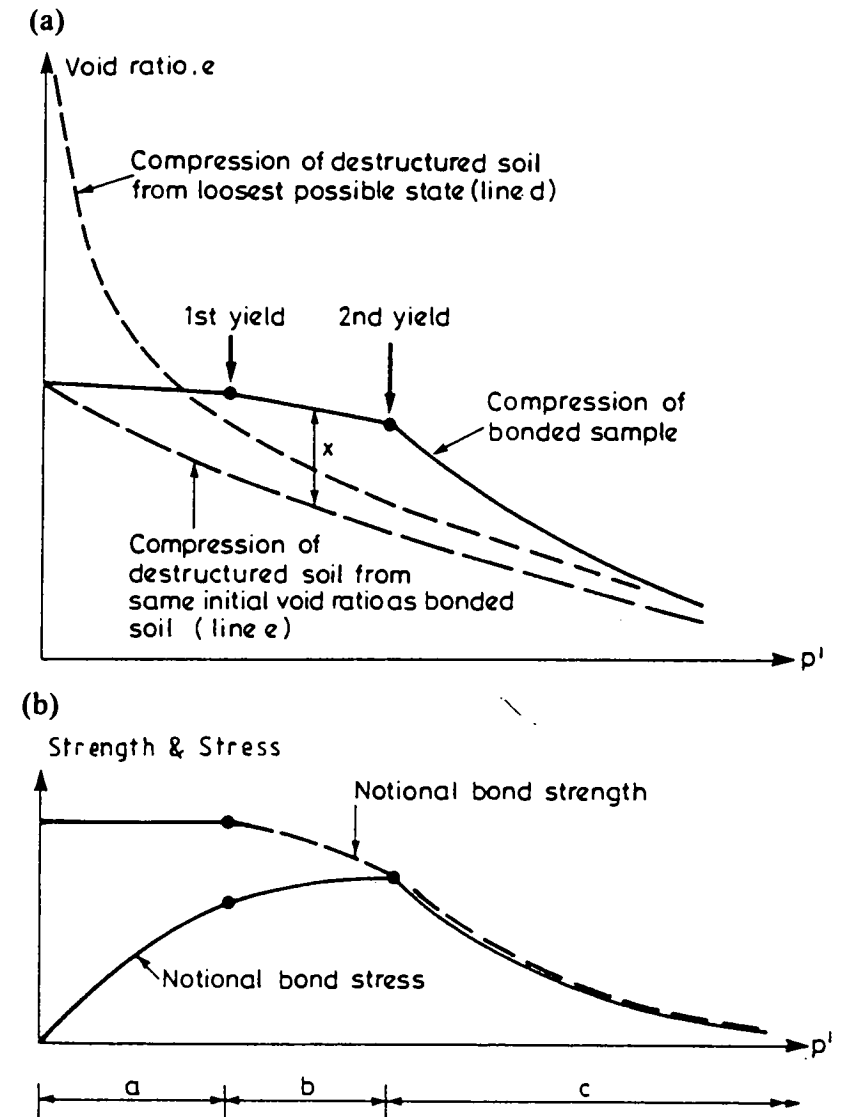
Figure 19-4 shows a conceptual description of soil behavior for a weakly bonded soil. In Figure 19-4(a), void ratio, e , versus mean effective stress, p' , the solid curve represents an oedometer test on a weakly bonded specimen. The dashed curve labeled *d* represents the compression curve from a loosest initial condition of the destructured soil, whereas the dashed curve *e* represents the compression curve for a destructured soil with an initial void ratio equal to that of the weakly bonded specimen. The weakly bonded specimen experiences no compression until it reaches the first yield point. Figure 19-4(b) provides a hypothesized comparison of bond strength with interparticle stress. At the first yield point the bond strength starts to drop because small interparticle strains weaken bonds, whereas at the second yield point the bond stress equals the bond strength, and bonds start breaking. The curves of reference void ratio e versus effective stress p' in Figure 19-4 provide boundaries for classifying soil behavior. When soils have p', e states that plot below the loosest destructured curve (labeled *d*), they behave as stable soils. When they plot above that curve, they behave as metastable soils.

Although this classification system does not currently provide quantitative correlations with shear strength, in the future it may provide a more

effective framework for empirical correlations than do Atterberg limits, which effectively describe transported soil properties. Vaughan et al. (1988) made several important observations concerning evaluations of shear strength of saprolites. The small strains induced during sampling may weaken bonds and lower the shear-strength values measured in the laboratory. In addition, residual soils often cannot sustain high capillary suctions, and the resulting unloading experienced during sampling causes expansion and breaks bonds. Finally, the laboratory-measured yield stresses are generally lower than those measured by in situ tests. Although these yield-stress values often prove valuable for evaluating deformations, the entire failure envelope must be known in order to estimate safety against instability.

Brand (1985) suggested that bonding causes saprolites at low effective stresses to have higher strengths than those predicted by triaxial tests run at high effective stresses and interpreted using a straight-line Mohr-Coulomb failure envelope. Figure 19-5 shows how the straight-line envelope can underestimate the actual curved failure envelope that applies at low effective stress. Vaughan (1985a) reported that weak bonding probably causes a small effective stress cohesion intercept, c' , that can be estimated from drained unconfined tests. Figure 19-6 shows that a horizontal stress path at constant q , $(\sigma_1 - \sigma_3)/2$, and decreasing p' , $(\sigma'_1 + \sigma'_3)/2$, corresponds to slope failures caused by rising pore pressures. Typical triaxial tests fail samples along the wrong stress path and result in unrealistically high p' values at failure.

Two additional factors that influence the shear strength of saprolites are the unsaturated state of the soil and relict joints. Lumb (1975) tested both saturated and unsaturated residual soil specimens in drained triaxial tests. He found that the straight-line envelopes determined from these tests gave drained friction-angle values (ϕ_d) that were independent of saturation, S , but that the drained cohesion values, c_d , showed a statistical correlation with saturation for soils derived from volcanic rhyolites and with saturation and void ratio for soils derived from granite. Lumb's test results showed that for all saprolites overlying granites, $\phi_d = 32$ degrees, whereas for unsaturated soils, $c_d = 0$ to 75 kPa and for saturated soils, $c_d = 0$ to 50 kPa. For saprolites overlying volcanic rocks, $\phi_d =$



36 degrees, whereas for unsaturated soils, $c_d = 60$ kPa and for saturated soils, $c_d = 25$ kPa. Sowers and Richardson (1983) reported the 67 percent confidence line for results of drained triaxial tests on both saturated and unsaturated specimens of saprolite derived from a range of different gneiss and schist parent rocks sampled during the design and construction of the Metropolitan Atlanta Rapid Transit Authority routes in Atlanta, Georgia. For saturated specimens, $\phi' = 32$ degrees and $c' = 0$ kPa, whereas for unsaturated specimens, $\phi' = 30$ degrees and $c' = 14$ kPa. The saprolites derived from igneous rocks in Hong Kong and those formed on metamorphic rocks in Georgia all have ϕ' values of 30 to 35 degrees but with widely vary-

FIGURE 19-4 Conceptual description of soil behavior for weakly bonded soil: (a) oedometer test on weakly bonded specimen; (b) comparison of bond strength with interparticle stress (Vaughan et al. 1988).

ing cohesion intercepts. The cohesion values represent an empirical fit to a curved envelope.

The cohesion intercept often represents an apparent cohesion resulting from capillary suction in the soils. Fredlund (1987) ran staged triaxial tests on unsaturated undisturbed saprolite specimens by setting constant values of total confining pressure,

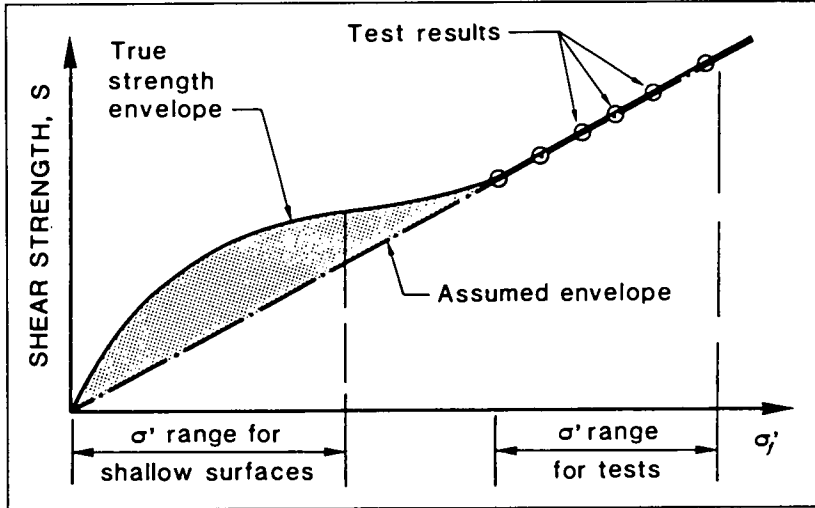


FIGURE 19-5 Underestimation of shear strengths because of incorrect strength envelope deduced from data obtained at too high normal stresses (Brand 1985). REPRINTED FROM PROCEEDINGS OF THE 11TH INTERNATIONAL CONFERENCE ON SOIL MECHANICS AND FOUNDATION ENGINEERING, SAN FRANCISCO, 12-16 AUGUST 1985, VOLUME 5, 1985-1988, 3153 PP., 5 VOLS., A.A. BALKEMA, OLD POST ROAD, BROOKFIELD, VERMONT 05036

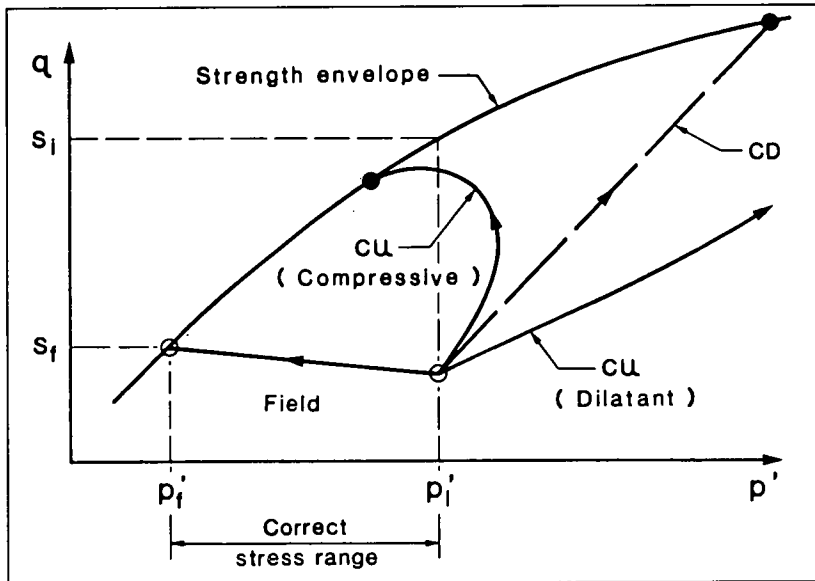


FIGURE 19-6 Comparison between stress paths for rain-induced slope failure and for triaxial tests (Brand 1981). REPRINTED FROM PROCEEDINGS OF THE 10TH INTERNATIONAL CONFERENCE ON SOIL MECHANICS AND FOUNDATION ENGINEERING, STOCKHOLM, 15-19 JUNE 1981, VOLUME 3, 1981-1982, 3542 PP., 4 VOLS., A.A. BALKEMA, OLD POST ROAD, BROOKFIELD, VERMONT 05036

σ , pore-air pressure, u_a , and pore-water pressure, u_w , and then measuring the deviator stress while shearing the specimens at a constant strain rate of 0.001 to 0.004 percent per minute. Fredlund increased the deviator stress until it reached a clear peak, unloaded the sample, adjusted σ and u_a while maintaining u_w constant, and then sheared the specimen again. Figure 19-7 shows the results for a multistage test performed on a decomposed granite specimen taken from a Hong Kong slope. The shear strength can be described by the following equation:

$$\tau = c + (\sigma - u_a) \tan\phi' \tag{19.1}$$

In the above equation, the cohesion, c , depends upon both the effective stress cohesion intercept, c' , and the matrix suction, $u_a - u_w$, according to the following equation:

$$c = c' + (u_a - u_w) \tan\phi^b \tag{19.2}$$

The ϕ' value equals the slope of envelopes tangent to Mohr circles plotted on τ versus $(\sigma - u_a)$ axes and equals 33.4 degrees for the tests shown in Figure 19-7. These tests were run at a constant $(\sigma_3 - u_a)$ of 140 kPa. The slope of the c versus $(u_a - u_w)$ plot, ϕ^b , equals 16.2 degrees, and the intercept, c' , equals 43 kPa.

Abramanto and Carvalho (1989) ran multistage drained triaxial tests on unsaturated specimens of weathered migmatites from the Serra do Mar region of Brazil at $(\sigma_3 - u_a)$ of 10 kPa. They used a curved line to determine the cohesion intercept, c , in kilopascals by the following equation:

$$c = 2.5 (u_a - u_w)^{0.5} \tag{19.3}$$

These test results suggest that c' equals 0.0. Both of these descriptions show that the shear strength of unsaturated saprolites depends upon three stress variables. Unfortunately, using this description in stability calculations means that the in situ matrix suction, $(u_a - u_w)$, must be measured or predicted.

Relict joints represent the final element influencing the mass shear strength of saprolites. Sandroni (1985) divided discontinuities into three classes according to their size. *Relict structures* represent faults, joints, dikes, and lithological contacts that range in dimension from meters to tens of meters. *Macrostructures* are visible to the naked eye and range in size from centimeters to 1 to 2 m. Isotropic macrostructures can be described as monotonous, stained, veiny, mottled, or porous, and anisotropic macrostructures can be described as

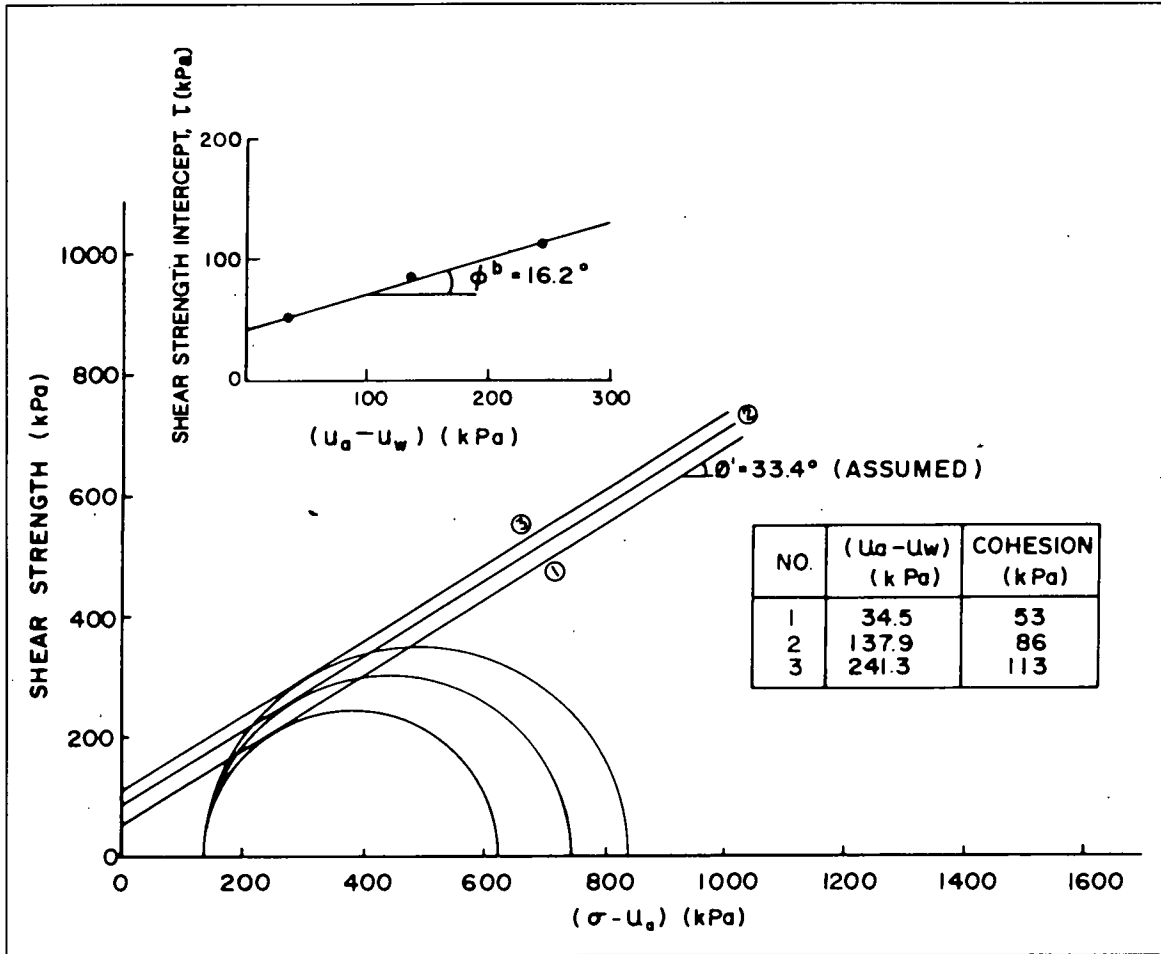


FIGURE 19-7
Mohr circles and
determination of ϕ^b
for decomposed
Hong Kong granite
(Fredlund 1987).
REPRINTED WITH
PERMISSION OF JOHN WILEY
& SONS, LTD.

laminated, banded, schistose, lenticular, or folded. Other macrostructures include remnants, cavities, and concretions. Finally, *microstructures* range from microns to tens of millimeters and can be viewed only by either a hand lens or a microscope.

All three discontinuity types can significantly reduce the mass shear strength below values measured in small-sized laboratory specimens. St. John et al. (1969) described the thin black seams often found in residual soils derived from igneous and metamorphic rocks. The undrained shear strength measured on 10-cm-diameter specimens of saprolite overlying gneiss with black seams oriented at 45 degrees was 50 to 67 percent of the undrained shear strength measured on intact specimens. These black seams had visible slickensides, suggesting previous displacements. Boyce (1985) ran ring-shear tests on tropical residual soils to measure the limiting residual shear strength controlling such slickensided surfaces. When he plotted ϕ^b values versus either clay fraction or plasticity index, he found that his results plotted both above

and below the measured values of ϕ^b for sedimentary soils. Decomposed phyllites had lower ϕ^b values than sedimentary soils of equal clay fraction, and volcanic soils containing allophane and halloysite had higher ϕ^b values.

3. PORE PRESSURES

Rainfall frequently triggers landslides in residual soils. Figure 19-8 shows how rainfall infiltration can increase positive pore pressures by raising either a perched or a regional water table. Townsend (1985) reported that for some naturally occurring residual soils with field permeabilities of 10^{-4} to 10^{-5} cm/sec, compaction decreased the permeability to 10^{-5} to 10^{-7} cm/sec. Brand (1985) added that naturally occurring highly transmissive zones, or pipes, in residual soils can make mass permeabilities very high. Therefore pore pressures in residual soil slopes often react quickly to heavy rainfall. Figure 19-9 shows that heavy rainfall for two days raised the measured piezometric head in a Hong

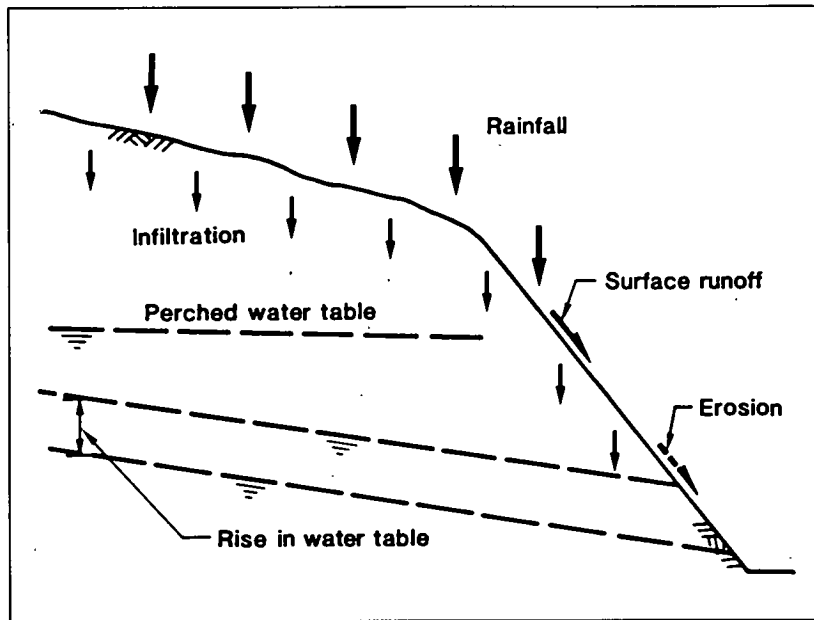
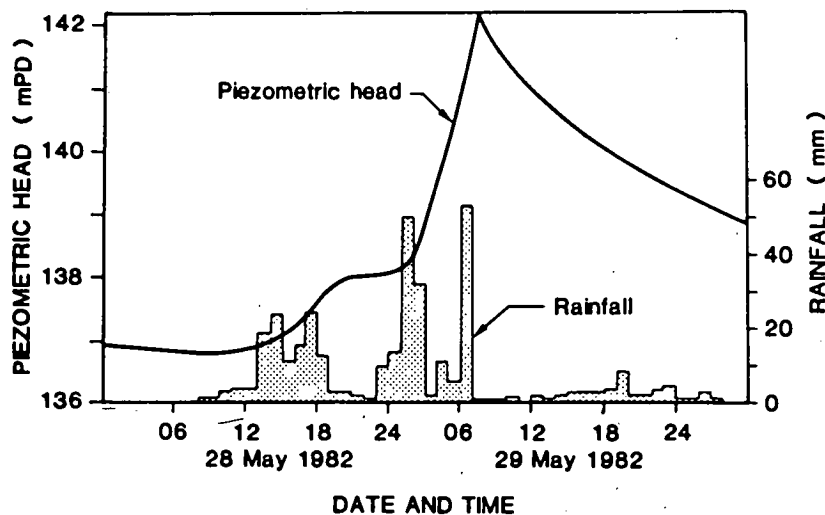


FIGURE 19-8
(above)
Diagrammatic
representation of
effects of rainfall on
slope (Brand 1985).

REPRINTED FROM
PROCEEDINGS OF THE 11TH
INTERNATIONAL
CONFERENCE ON SOIL
MECHANICS AND
FOUNDATION
ENGINEERING, SAN
FRANCISCO, 12-16 AUGUST
1985, VOLUME 5, 1985-1988,
3153 PP., 5 VOLS., A. A.
BALKEMA, OLD POST ROAD,
BROOKFIELD, VERMONT
05036

Kong slope 5 m in only 18 hr, and the piezometric head dropped quickly when the rains stopped. Such rapid changes make it difficult to measure pore pressures in residual soil slopes at the point of slope failure. Either automatic-reading piezometers or a system that can record the highest rise during and following heavy rainfall is required. Brand (1985) described a series of small Halcrow buckets chained together and suspended in an open-standpipe piezometer. The highest water-level rise is recorded by measuring the depth to the highest filled bucket.

Shallow failures can occur on slopes composed of unsaturated saprolite when rainfall infiltration eliminates the suction and lowers the apparent



cohesion. Lumb (1962) proposed that a wetting front advances during heavy rainfall, as shown in Figure 19-10. During a rainfall exceeding the infiltration capacity of the soil for time t , the front will advance a distance h , as given by the following equation:

$$h = \frac{kt}{n(S_f - S_o)} \quad (19.4)$$

where h and t are as defined previously and

k = coefficient of permeability,

n = porosity,

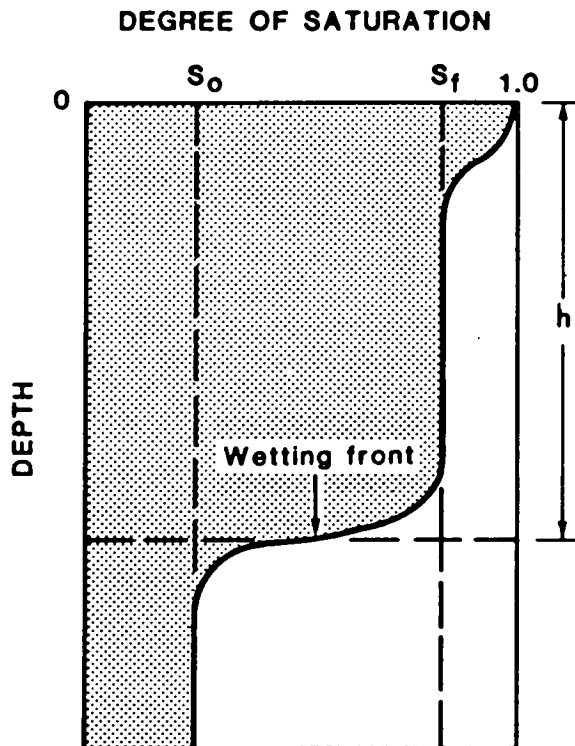
S_f = final saturation, and

S_o = initial saturation.

Equation 19.4 suggests that the wetting front advances faster when antecedent rainfall has increased S_o . Lumb (1975) reported that decomposed volcanic soils have an effective mass permeability equal to 1.5×10^{-4} cm/sec and that if the rainfall rate exceeds 130 mm/day for a three-day period, providing a total accumulation of about 400 mm, the wetting front will advance 4 m into the soil. The mass permeability in decomposed granite equals 8.0×10^{-4} cm/sec and the same 400 mm of rain needs to accumulate within a 14-hr period to advance the wetting front 4 m. Vaughan (1985b) demonstrated by simple analysis that a profile that has continuously decreasing permeability with depth can lead to instability, whereas increasing permeability with depth provides natural drainage. Although Lumb and Vaughan have analyzed vertical infiltration into slopes, these methods do not automatically provide a good quantitative prediction method for many specific slopes.

Brand (1985) evaluated the current ability to predict the performance of residual soil slopes. He reported that there are good methods of analysis and that it is possible to predict failure modes based upon observed failures in similar slopes and to estimate shear strength fairly well but it is not possible to effectively estimate pore pressures at the point of incipient slope failure. Because there is only a poor to fair ability to predict slope performance, design practices often depend upon empirical and semiempirical methods. For example, four design approaches have been used in Hong Kong:

- Correlation of slope failures with rainfall pattern,
- Terrain evaluation using geomorphological mapping,



- Semiempirical methods developed from evaluation of past failures, and
- Soil mechanics analysis.

In Hong Kong soil mechanics analyses are used most often to evaluate remedial measures for correcting or stabilizing slope failures and for analyzing the stability of cut slopes that are next to critical structures. The other three methods are used for land use planning and for designing cut slopes along transportation routes.

4. CASE HISTORIES

Case histories of slope stability analyses for slopes in residual soils are widely dispersed throughout the technical literature. Also, as noted in the previous sections of this chapter, residual soils may exhibit a considerable range in properties, and experience gained in one region should be used with caution in others. In the following sections some of the issues discussed earlier in this chapter are illustrated briefly with case histories from Brazil, Hong Kong, and the state of North Carolina in the United States. These examples begin to demonstrate the regional differences in residual

soils and some of the similarities of the factors leading to slope instability in residual soils.

4.1 Brazil

Vargas and Pichler (1957) described residual soil and rock landslides occurring in Santos, Brazil. They divided the landslides occurring in Brazil into three classes:

- Class 1 landslides involve creep of surficial residual soil,
- Class 2 slides involve detritus (colluvium) at lower elevations in old slide areas, and
- Class 3 slides involve sudden rupture of residual soil overlying bedrock.

At Monte Serrate, a 50-m-high Class 3 landslide occurred in February 1928 when 720 mm of rain fell during the month. This landslide was back analyzed using standard soil-stability analysis methods for circular failure surfaces. The results showed that failure occurred when the pore pressure ratio, r_u , reached 0.35 if $\phi = 42$ degrees and $c = 39$ kPa, as measured in direct shear tests. Da Costa Nunes et al. (1979) provided a wider overview of landslides found in Brazil and divided slides into classes according to their geological regions. Vargas (1974) concluded that rotational or planar slides in residual soils fail at the end of the rainy season either during or following rainfall more intense than 100 mm/day. More severe and faster-moving flows that remove the residual soil mantle fail during catastrophic rainstorms with intensities greater than 50 mm/hour.

Jones (1973) reported on some especially severe landslides that occurred over a 100-km² area along the Serra das Araras escarpment, a subdivision of Serra do Mar; these landslides killed an estimated 1,700 people. On January 22 and 23, 1967, 250 mm of rain fell during 3.5 hr and triggered more than 10,000 shallow landslides classified as debris avalanches, debris flows, and mud flows. These landslides removed from less than 1 m to up to several meters of residual soil overlying the well-banded biotitic, feldspathic, and garnetiferous gneisses that were cut by aplitic veins and diabase dikes. The weathering profiles showed an abrupt transition between the Zone IC and Zone IIA materials and the Zone III materials. Specimens taken from the landslide area were classified

FIGURE 19-10 Representation of advance of wetting front as water infiltrates soil (Lumb 1975).

FIGURE 19-9 (opposite page) Rapid changes in groundwater table measured in Hong Kong slope (Brand 1985).

REPRINTED FROM PROCEEDINGS OF THE 11TH INTERNATIONAL CONFERENCE ON SOIL MECHANICS AND FOUNDATION ENGINEERING, SAN FRANCISCO, 12-16 AUGUST 1985, VOLUME 5, 1985-1988, 3153 PP., 5 VOLS., A.A. BALKEMA, OLD POST ROAD, BROOKFIELD, VERMONT 05036

according to the Unified Soil Classification System as low-plasticity silts and sandy silts (ML and SM-ML).

Wolle and Hachich (1989) quantitatively evaluated translational landslides occurring in the same Serra do Mar region. The weathering profile typically had 1 to 1.5 m of colluvial cover overlying 1 to 2 m of saprolite that, in turn, overlaid migmatites. Open fractures in the Zone IIA transition material made the mass permeability high, and the water table occurred at depths of 20 to 30 m in the fractured bedrock. Dense vegetative cover intercepted infiltration and prevented erosion. Observed landslides occurred on the 40- to 45-degree slopes and were 7 to 25 m wide, over 100 m long, and about 1 m deep. The threshold precipitation in this region equaled 180 mm/day when antecedent rain had moistened the soil. The relatively high permeabilities averaged 5×10^{-4} cm/sec, and during intense rainfall the wetting front advanced 1.0 to 1.5 m into the soil profile in 4 to 12 hr. During the rainy season, soils had saturation values of 60 to 80 percent, whereas laboratory tests suggested that no suction occurred when saturations reached 92 to 95 percent. Calculations showed that the slopes failed when rainfall infiltration decreased suctions at a 1-m depth to values ranging from 1 to 2 kPa. Measurements during the rainy season suggested suctions of 1 to 10 kPa. Wolle and Hachich also estimated the influence of root strength on stability and concluded that the sliding soil must reach a width of at least 6 to 15 m before overcoming root reinforcement. In general, it seems that these land-

slides support Lumb's (1975) proposed hypothesis that landsliding is caused by the advance of a wetting front during intense and sustained rainfall.

4.2 Hong Kong

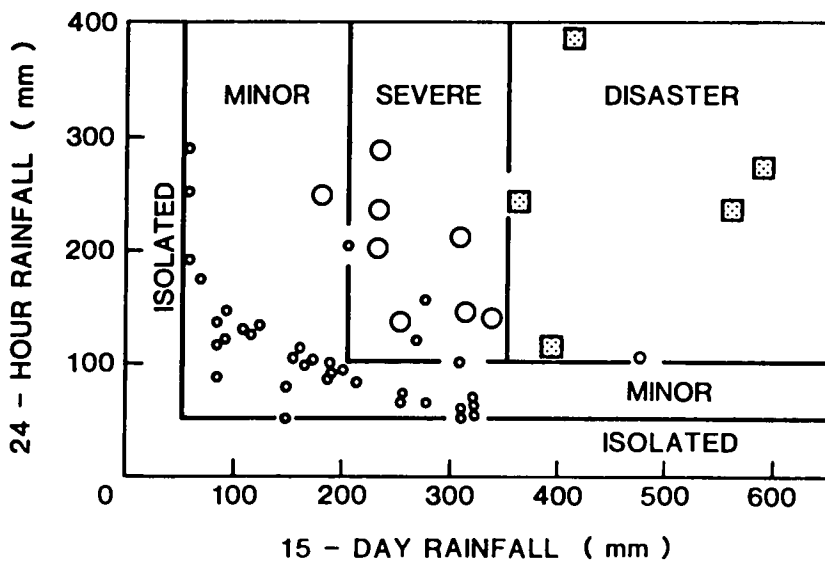
Lumb (1975) examined slope failures in Hong Kong and correlated their occurrence with rainfall intensity. He divided rainfall events into four categories:

- *Disastrous events* causing more than 50 recorded landslides in one day,
- *Severe events* causing 10 to 50 landslides in one day,
- *Minor events* causing fewer than 10 landslides, and
- *Isolated events* causing only a single slip.

Figure 19-11 shows these rainfall events plotted as the 24-hr rainfall versus the 15-day antecedent rainfall. Using rainfall data obtained from records of the Royal Observatory, Lumb identified bounds between different levels of event severity. Disastrous events occurred when the 24-hr rainfall exceeded 100 mm and the 15-day antecedent rainfall exceeded 350 mm. Severe events were triggered by rainfall of 100 mm/day following 200 mm of antecedent rainfall.

Lumb (1975) divided the Hong Kong landslides into three types. All three types are landslides that are generally less than 3 m deep and have a thickness-to-length ratio of less than 0.15. Type 1 landslides represent fill embankments constructed over residual soil; these move following heavy rainfall. Type 2 landslides occur in natural residual soil or colluvium, extend to or beyond the crest of the slope, and fail following heavy rainfall. The Type 2 failures generally occur in decomposed volcanics but move more slowly than the Type 1 saturated fills. Type 3 landslides occur within a cut face, do not extend beyond the crest of the slope, and often occur in areas of decomposed granite. Type 3 failures occasionally occur during dry periods when some other water source saturates the decomposed granite. Type 3 failures are smaller and much less destructive than either the Type 1 or Type 2 landslides. Lumb (1975) also described two much deeper landslides that differ from his three primary types. These last two moved more slowly and involved seepage patterns much more complex than simple vertical rainfall infiltration.

FIGURE 19-11
Relationship
between rainfall and
landslides in Hong
Kong (Lumb 1975).



Brand (1985) further examined the landslide risk in Hong Kong using three distinct methods. He first reexamined the earlier correlations by Lumb (1975) using data collected from 46 automatic recording rain gauges distributed throughout Hong Kong and considered 1-hr rainfalls, 24-hr rainfalls, and antecedent rainfall for periods varying up to 30 days. In addition, he identified the precise time of landslide events by using the Fire Services Department reports of calls. Figure 19-12 shows average landslides per day and average casualties per day plotted versus maximum hourly rainfall. This plot shows a clear threshold of 70 mm/hour of rainfall to trigger multiple landslides with subsequent loss of life. Brand (1985) concluded that localized short-duration rainfalls caused the majority of landslides and that antecedent rainfall had little influence. He further concluded that in Hong Kong storm intensities greater than 70 mm/hour trigger landslides and that daily rainfalls of greater than 100 mm/day often indicate that a short intense rainfall has occurred during that day.

The third landslide prediction method investigated by Brand (1985) is based on semiempirical charts and requires detailed data on the height and angle of slopes. Figure 19-13 shows a semiempirical plot developed from a study of 177 slopes, including failed slopes (solid circles) and unfailed slopes (open circles). Solid lines portray the progression of Hong Kong's design guidelines over the years. In 1950 slopes were cut at 75 degrees, or $1(H):4(V)$, whereas in more recent guidelines the design slope angle depends upon slope height. This plot clearly shows that for cut slopes in residual soils, traditional stability analyses lead to flatter slopes than those recommended by existing semiempirical design practices.

Both Lumb (1975) and Brand (1985) provided detailed geotechnical information necessary to analyze the performance of individual slopes. However, as described earlier, limitations in predicting pore pressures at the point of incipient failure make these stability predictions uncertain. Figure 19-14 shows typical Hong Kong soil profiles overlying both granites and volcanics. The granites can decompose to depths greater than 30 m and the unweathered granite has joint spacings of 2 to 10 m. The water table typically is found near the upper surface of the unweathered rock; thus the full soil profile can be unsaturated. Only the

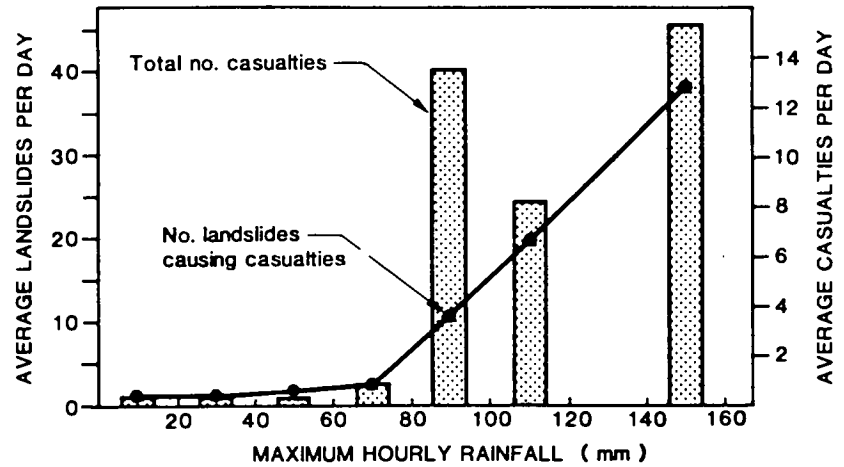


FIGURE 19-12 Number of landslides causing casualties and number of casualties for period 1963–1983 in Hong Kong compared with maximum hourly rainfall (Lumb 1975).

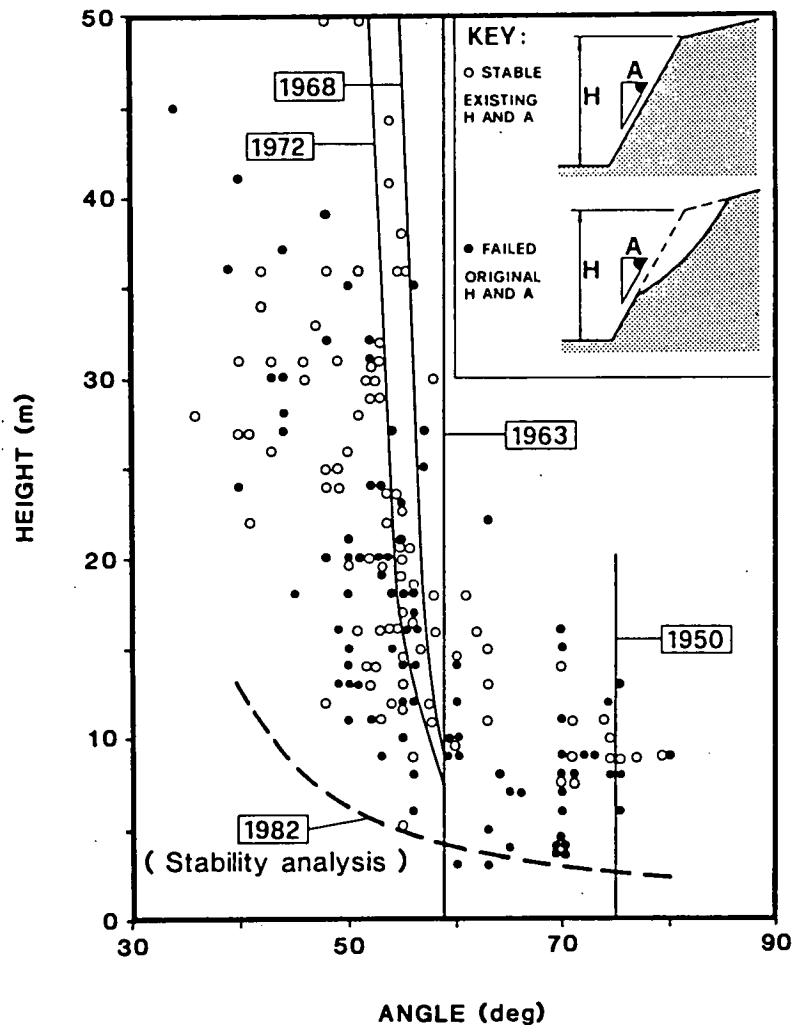


FIGURE 19-13 Relationship between height and slope angle for 177 Hong Kong cut slopes (Brand and Hudson 1982).

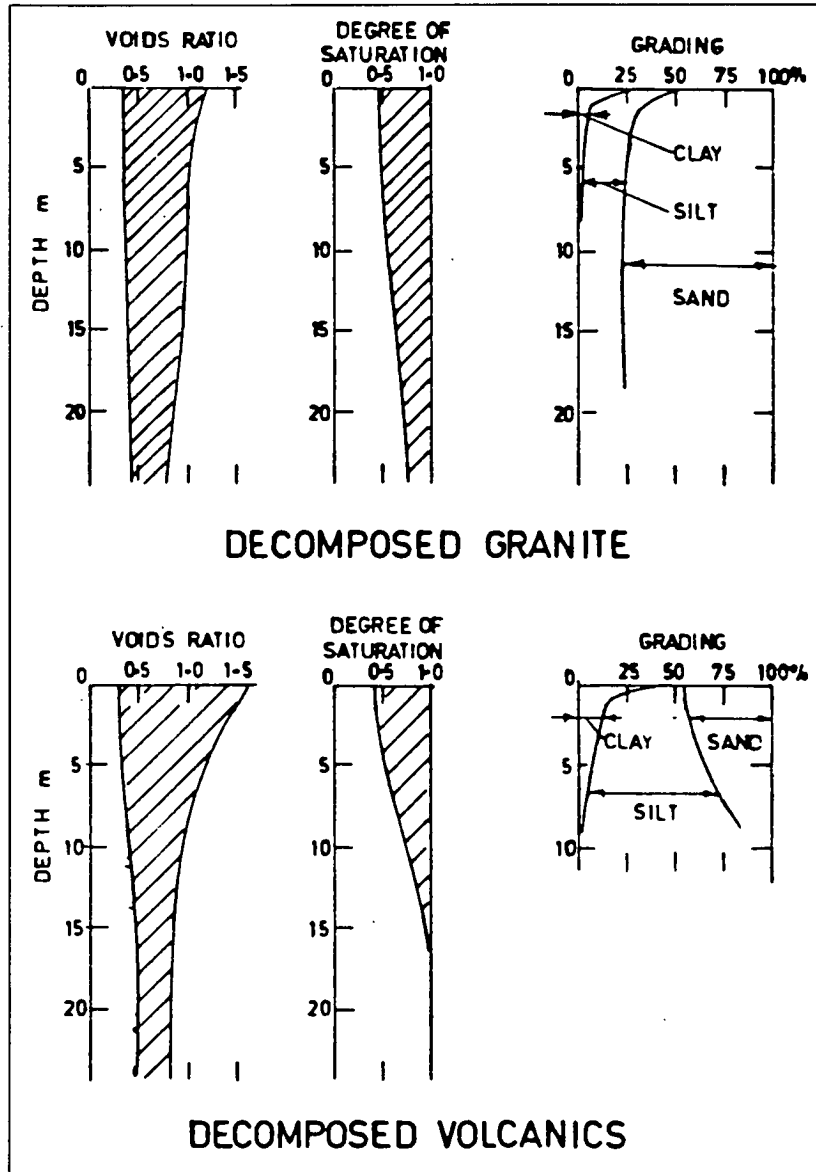


FIGURE 19-14
Bulk properties of
Hong Kong residual
soils (Lumb 1975).

top few meters of soil show any clay fraction, and the soils are classified as silty sands. The volcanics have closer joint spacings of 0.2 to 1 m and typically weather to depths of 10 m, rarely more than 20 m. These soils are classified as sandy silts and have slightly higher void ratios. Colluvium covers the residual soils on the lower slopes. Colluvium overlying decomposed granites has a similar texture to the residual soils, whereas the colluvium overlying the volcanics has more rounded cobbles and small core stones than the underlying residual soils. Lumb (1975) measured an average coefficient of permeability of 8.0×10^{-4} cm/sec in decomposed granites by both field in situ tests

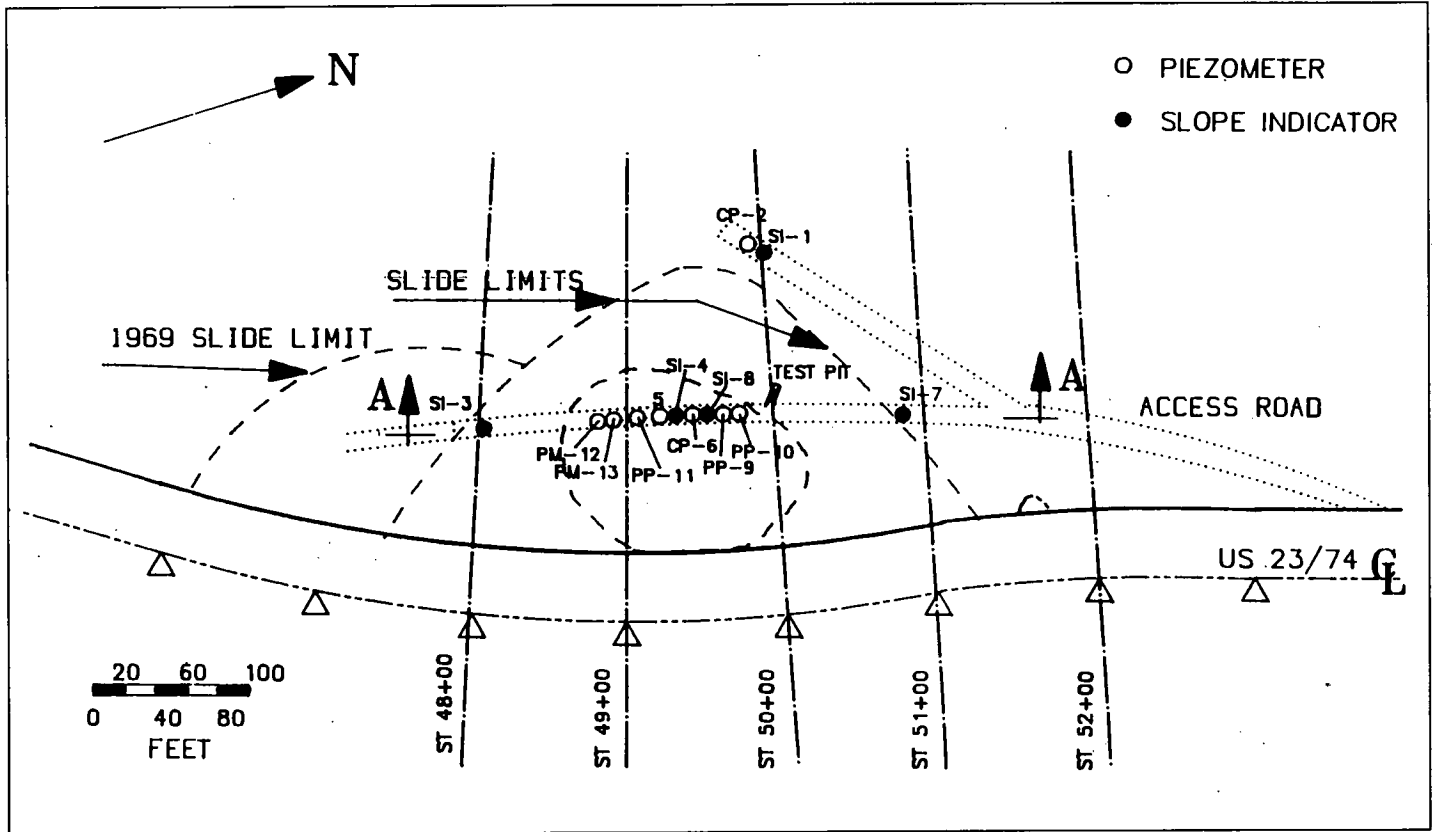
and laboratory tests on undisturbed specimens. Because the volcanics have a closer joint spacing, their average field-measured permeability was 1.5×10^{-4} cm/sec, some two orders of magnitude greater than the average permeability value for these volcanic materials measured in the laboratory, which was 2.0×10^{-6} cm/sec.

Brand (1985) analyzed six specific landslides for which field investigations determined the existing slope geometry and underlying soil profiles and laboratory testing determined the shear strength. Three cases (numbered 1 to 3) involved slopes that had not failed, but their calculated factors of safety ranged from 0.80 to 0.95. Three additional cases (numbered 4 to 6) involved slopes that had failed, but their calculated factors of safety ranged from 1.24 to 1.30. In the first three cases, Brand concluded that either the acting strengths or the suctions were larger than those used in the stability analyses. In Case 4 the actual weathered soil depth was greater than expected from the preliminary borings. In Case 5 sliding occurred along slickensided relict joints, and in Case 6 subvertical relict joints encouraged vertical seepage and influenced the observed failure mode. Therefore, in all these cases, the exploration either did not correctly determine the soil weathering profile or did not accurately identify soil strength properties or groundwater conditions.

4.3 North Carolina

The North Carolina Department of Transportation has experienced recurring landslides at their highway cuts. In 1987 and 1988 two landslides were investigated to better define the failure mode, the acting shear strength, and the pore pressures at the point of slope failure for use in future designs (Lambe and Riad 1991). These two landslides, known as the Balsam Gap landslide and the Boone landslide, were both slow-moving and required no immediate repair. Both landslides moved along shear surfaces just below the colluvium-saprolite interface. Piezometers installed at both sites measured zero or negative pore pressures acting on the shear surfaces.

Figure 19-15 shows a plan view of the Balsam Gap landslide and locates the borings made to take samples and install instrumentation. This 1.75(H):1(V) slope had been excavated north of US 23/74. The slope started moving in 1980 and



involved a failure volume of 15 000 m³. Rainfall during the years from 1979 to 1988 averaged 1140 mm/year, but only monthly rainfall data were available from nearby rainfall recording stations. Figure 19-16 shows the cross section and soil profile that were determined from borings and a test pit. The test pit was excavated to examine the 5-mm-thick slickensided shear surface located just below the colluvium cover. The interface between the saprolite's rocklike structure and the colluvium's thoroughly mixed appearance was readily identified.

The residual soil overlaid coarse granitic gneiss bedrock. Figure 19-17 shows the soil profile based upon the Standard Penetration Test profile in Boring 4 and tests on tube samples taken from Borings 5 and 6. The colluvium was classified as a sandy clay (CL-ML), and the saprolite was classified as a silty sand (SM). Falling-head permeability tests performed on trimmed consolidation specimens measured an average permeability of 3×10^{-4} cm/sec for the saprolite and a permeability of 2×10^{-7} cm/sec for the colluvium. Therefore, the colluvium acted as a low-permeability cap over the saprolite. Drained direct-shear tests on the saprolite

measured three envelopes of the type proposed by Skempton (1970). For the fully softened envelope, $\phi' = 27$ degrees and $c' = 19$ kPa. Analyzing non-circular failure surfaces, such as the one shown in Figure 19-16, resulted in the resistance envelopes in Figure 19-18. A resistance envelope portrays the average shear stress and average effective normal stress acting along a family of failure surfaces for an assumed pore-pressure distribution (Casagrande 1950). Lacking any measured pore pressures during heavy rainfall, resistance envelopes were calculated for three different pore-pressure levels:

- $r_u = 0.0$ was used to establish a lower bound,
- $r_u = 0.25$ was used to provide information on "average" conditions, and
- $r_u = 0.5$ was used to establish an upper bound.

These back analyses suggest that the failures may be explained by $r_u = 0.32$, with fully softened shear strength acting along the failure surface shown in Figure 19-16 and with an average effective normal stress along the failure surface of 48 kPa.

The weathering profile of the Boone landslide differed from the profile at Balsam Gap because a

FIGURE 19-15 Plan view of Balsam Gap landslide (Lambe and Riad 1991).

REPRINTED WITH PERMISSION OF AMERICAN SOCIETY OF CIVIL ENGINEERS

FIGURE 19-16
 Cross section of
 Balsam Gap
 landslide (Lambe
 and Riad 1991).
 REPRINTED WITH
 PERMISSION OF
 AMERICAN SOCIETY OF
 CIVIL ENGINEERS

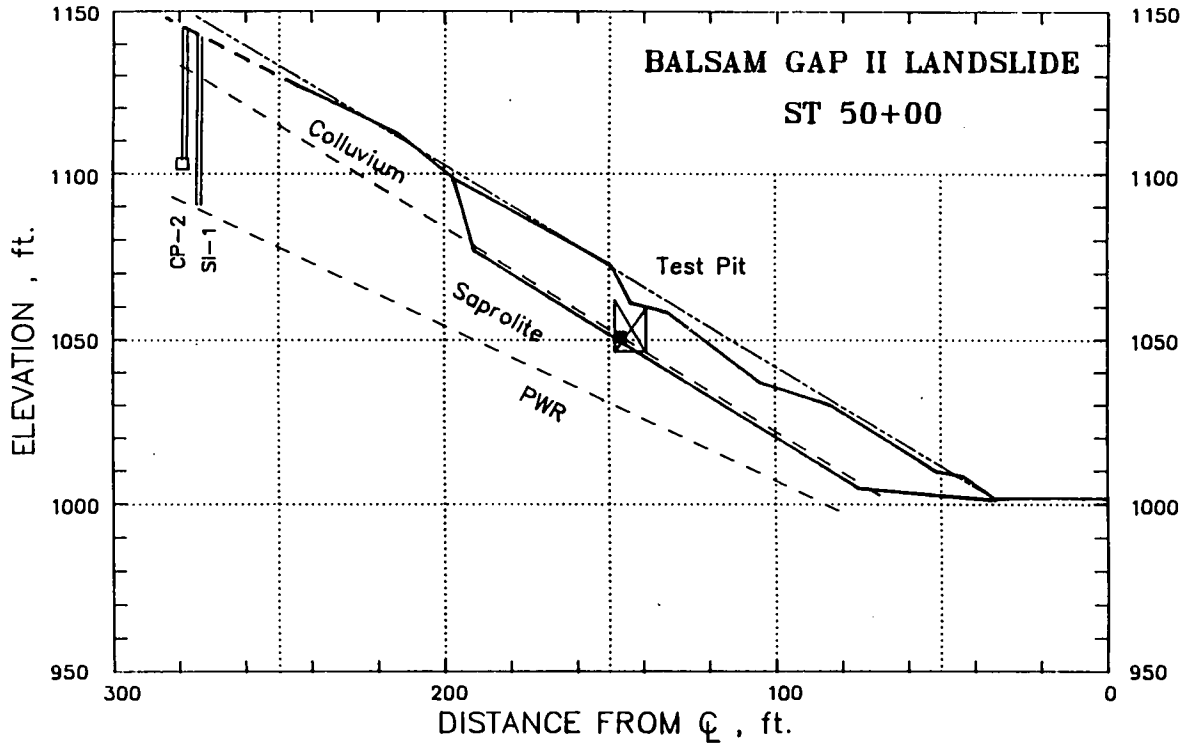
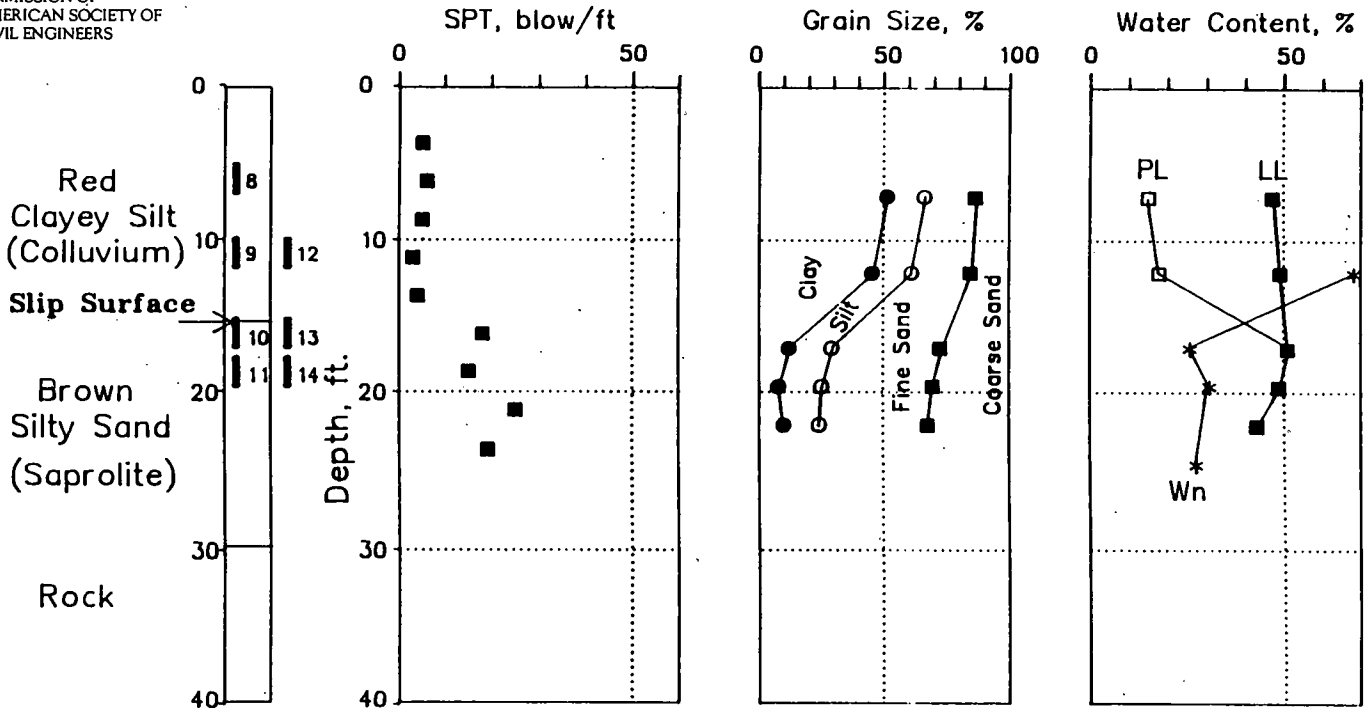


FIGURE 19-17
 (below)
 Data from Balsam
 Gap landslide
 boring SI-4 (Lambe
 and Riad 1991).
 REPRINTED WITH
 PERMISSION OF
 AMERICAN SOCIETY OF
 CIVIL ENGINEERS



(Samples from borings 5 and 6)

more pervious colluvium covered the saprolite and the saprolite had weathered from a biotitic-granitic gneiss. The saprolite was classified as a silt and had an average permeability of 1×10^{-5} cm/sec. Gravel- and cobble-sized particles prevented sampling of the colluvium, which appeared more pervious than the underlying saprolite. Vertical rainfall infiltration through the colluvium could have caused a perched water table on the saprolite. The shear surface was 300 mm thick and appeared as a wet seam at the top of the saprolite, in contrast to the clearly slickensided surface found at Balsam Gap. Back analyses suggested that failure occurred when r_u reached 0.24 and the shear strength fell to the residual envelope with $\phi' = 29$ degrees and $c' = 2$ kPa. At failure, the average effective normal stress, σ'_n , equaled 19 kPa.

For these two slow-moving landslides, the best information came from excavated test pits that intersected the failure surface from which block samples of the failure surface were obtained and trimmed so that the failure surface could be visually inspected and tested in the laboratory. Necessary safety precautions must be taken before entering such test pits, and temporary portable shoring, such as aluminum hydraulic shoring, should be used to hold the trenches open.

REFERENCES

- Abramento, M., and C.S. Carvalho. 1989. Geotechnical Parameters for the Study of Natural Slopes Instabilization at "Serra do Mar", Brazil. In *Proc., 12th International Conference on Soil Mechanics and Foundation Engineering*, Rio de Janeiro, A.A. Balkema, Rotterdam, Netherlands, pp. 1599-1602.
- Boyce, J.R. 1985. Some Observations on the Residual Strength of Tropical Soils. In *Proc., First International Conference on Geomechanics in Tropical Lateritic and Saprolitic Soils*, Brasilia, Brazil, Vol. 1, pp. 229-237.
- Brand, E.W. 1981. Some Thoughts on Rain-Induced Slope Failures. In *Proc., 10th International Conference on Soil Mechanics and Foundation Engineering*, Stockholm, Sweden, A.A. Balkema, Rotterdam, Netherlands, Vol. 3, pp. 373-376.
- Brand, E.W. 1985. Predicting the Performance of Residual Soil Slopes. In *Proc., 11th International Conference on Soil Mechanics and Foundation Engineering*, San Francisco, A.A. Balkema, Rotterdam, Netherlands, Vol. 5, pp. 2541-2578.
- Brand, E.W., and R.R. Hudson. 1982. Chase—An Empirical Approach to the Design of Cut Slopes in Hong Kong Soils. In *Proc., Seventh Southeast Asian Geotechnical Conference*, Hong Kong, Vol. 1, pp. 1-16.
- Brand, E.W., and H.B. Phillipson. 1985. Review of International Practice for Sampling and Testing of Residual Soils. In *Sampling and Testing of Residual Soils* (E.W. Brand and H.B. Phillipson, eds.), Scorpion Press, Hong Kong, pp. 7-21.
- Bressani, L.A., and P.R. Vaughan. 1989. Damage to Soil Structure during Triaxial Testing. In *Proc., 12th International Conference on Soil Mechanics and Foundation Engineering*, Rio de Janeiro, Brazil, A.A. Balkema, Rotterdam, Netherlands.
- Casagrande, A. 1950. Notes on the Design of Earth Dams. *Journal of the Boston Society of Civil Engineers*, Vol. 37, pp. 405-429.
- Da Costa Nunes, J.J., A.M.M. Costa Couto e Fonseca, and R.E. Hunt. 1979. Landslides of Brazil. In *Rockslides and Avalanches* (B. Voight, ed.), Elsevier Scientific Publishing Co., pp. 419-446.
- Deere, D.U., and F.D. Patton. 1971. Slope Stability in Residual Soils. In *Proc., Fourth Pan American Conference on Soil Mechanics and Foundation Engi-*

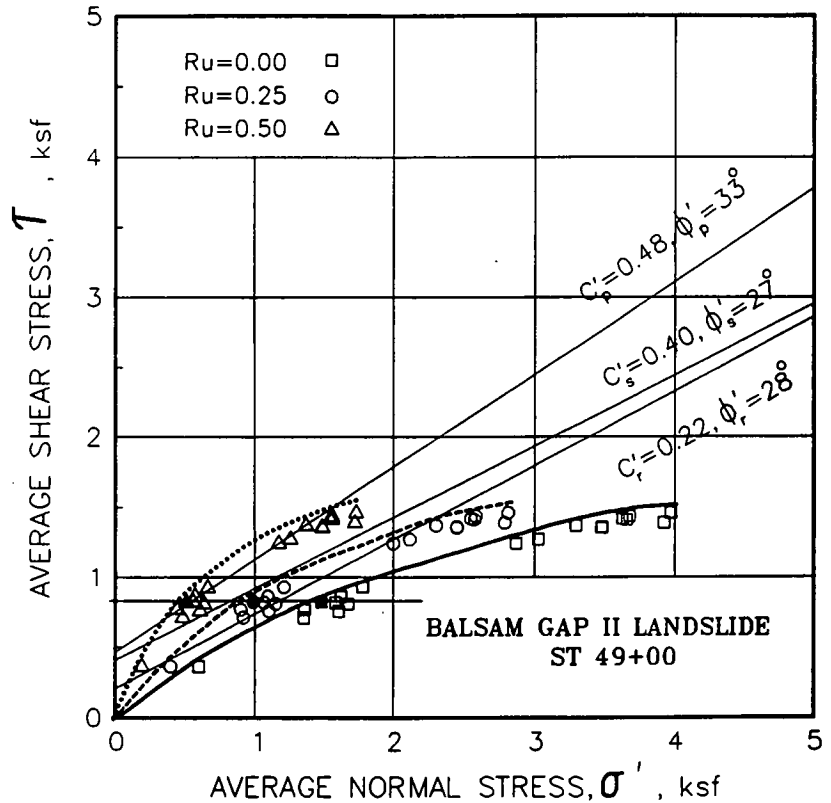


FIGURE 19-18
Resistance envelope
for Balsam Gap
landslide (Lambe
and Riad 1991).
REPRINTED WITH
PERMISSION OF
AMERICAN SOCIETY OF
CIVIL ENGINEERS

- neering, San Juan, Puerto Rico, American Society of Civil Engineers, New York, Vol. 1, pp. 87–170.
- De Mello, V.F.B. 1972. Thoughts on Soil Engineering Applicable to Residual Soils. In *Proc., Third Southeast Asian Conference on Soil Engineering*, Hong Kong, Hong Kong Institution of Engineers and Southeast Asian Geotechnical Society, pp. 5–34.
- Fredlund, D.G. 1987. Slope Stability Analysis Incorporating the Effect of Soil Suction. In *Slope Stability: Geotechnical Engineering and Geomorphology* (M.G. Anderson and K.S. Richards, eds.), John Wiley & Sons, New York, pp. 113–144.
- Geological Society of London. 1990. Tropical Residual Soils: Geological Society Engineering Group Working Party Report. *Quarterly Journal of Engineering Geology*, Geological Society of London, Vol. 23, No. 1, pp. 4–101.
- Jones, F.O. 1973. *Landslides of Rio de Janeiro and the Serra das Araras Escarpment, Brazil*. U.S. Geological Survey Professional Paper 697, 42 pp.
- Lambe, P.C., and A.H. Riad. 1991. Back Analysis of Two Landslides in Residual Soil. In *Proc., Ninth Pan American Conference on Soil Mechanics and Foundation Engineering*, American Society of Civil Engineers, New York, pp. 425–439.
- Lumb, P. 1962. Effect of Rain Storms on Slope Stability. In *Proc., Symposium on Hong Kong Soils*, Hong Kong, Hong Kong Joint Group of the Institutions of Civil, Mechanical, and Electrical Engineers, pp. 73–87.
- Lumb, P. 1975. Slope Failures in Hong Kong. *Quarterly Journal of Engineering Geology*, Geological Society of London, Vol. 8, pp. 31–65.
- Mitchell, J.K., and N. Sitar. 1982. Engineering Properties of Tropical Residual Soils. In *Engineering and Construction in Tropical and Residual Soils, Honolulu, Hawaii*, American Society of Civil Engineers, New York, pp. 30–57.
- Sandroni, S.S. 1985. Sampling and Testing of Residual Soils in Brazil. In *Sampling and Testing of Residual Soils* (E.W. Brand and H.B. Phillipson, eds.), Scorpion Press, Hong Kong, pp. 31–50.
- Skempton, A.W. 1970. First-Time Slides in Over-Consolidated Clays. *Geotechnique*, Vol. 20, No. 3, pp. 320–324.
- Sowers, G.F. 1954. Soil Problems in the Southern Piedmont Region. *Proc., ASCE*, Vol. 80, Separate No. 416.
- Sowers, G.F. 1963. Engineering Properties of Residual Soil Derived from Igneous and Metamorphic Rocks. In *Proc., Second Pan American Conference on Soil Mechanics and Foundation Engineering*, Brazil, American Society of Civil Engineers, New York, Vol. 1, pp. 39–61.
- Sowers, G.F., and T.L. Richardson. 1983. Residual Soils of Piedmont and Blue Ridge. In *Transportation Research Record 916*, TRB, National Research Council, Washington, D.C., pp. 10–16.
- St. John, B.J., G.F. Sowers, and C.E. Weaver. 1969. Slickensides in Residual Soils and Their Engineering Significance. In *Proc., Seventh International Conference on Soil Mechanics and Foundation Engineering*, Sociedad Mexicana de Mecánica de Suelos, Mexico City, Vol. 2, pp. 591–597.
- Townsend, F.C. 1985. Geotechnical Characteristics of Residual Soils. *Journal of the Geotechnical Engineering Division*, ASCE, Vol. 111, No. 1, pp. 77–94.
- Vargas, M. 1974. Engineering Properties of Residual Soils from the South-Central Region of Brazil. In *Proc., Second International Congress of the International Association of Engineering Geology*, Sao Paulo, Brazil, Associação Brasileira de Geologia de Engenharia, Vol. 1.
- Vargas, M., and E. Pichler. 1957. Residual Soil and Rock Slides in Santos (Brazil). In *Proc., Fourth International Conference on Soil Mechanics and Foundation Engineering*, Butterworths Scientific Publications, London, Vol. 2, pp. 394–398.
- Vaughan, P.R. 1985a. Mechanical and Hydraulic Properties of In-Situ Residual Soil General Report. In *Proc., First International Conference on Geomechanics in Tropical Lateritic and Saprolitic Soils*, Brasilia, Brazil, Comisión Federal de Electricidad, Mexico City, Vol. 3, pp. 231–263.
- Vaughan, P.R. 1985b. Pore Pressures due to Infiltration into Partially Saturated Slopes. In *Proc., First International Conference on Geomechanics in Tropical Lateritic and Saprolitic Soils*, Brasilia, Brazil, Comisión Federal de Electricidad, Mexico City, Vol. 2, pp. 61–71.
- Vaughan, P.R., M. Maccarini, and S.M. Mokhtar. 1988. Indexing the Engineering Properties of Residual Soil. *Quarterly Journal of Engineering Geology*, Geological Society of London, Vol. 21, pp. 69–84.
- White, R.M., and T.L. Richardson. 1987. Predicting the Difficulty and Cost of Excavation in the Piedmont. In *Foundations and Excavations in Decomposed Rock of the Piedmont Province* (R.E. Smith, ed.), American Society of Civil Engineers, New York, pp. 15–36.
- Wölle, C.M., and W. Hachich. 1989. Rain-Induced Landslides in Southeastern Brazil. In *Proc., 12th International Conference on Soil Mechanics and Foundation Engineering*, Brasilia, Brazil, A.A. Balkema, Rotterdam, Netherlands, pp. 1639–1642.